

Forced Vibration Tests of a Model Foundation on Rock Ground

N. Kasaki, M. Siota

Civil Engineering Dept., Kyushu Electric Power Co., Ltd., 2-1-82, Watanabedori, Chuo-ku, Fukuoka 810, Japan

M. Yamada, A. Ikeda, H. Tsuchiya, K. Kitazawa

Technical Research Institute, Taisei Corporation, 344-1, Nasemachi, Totsuda-ku, Yokohama 245, Japan

Y. Kuwabara, Y. Ogiwara

Nuclear Facility Engineering Dept., Taisei Corporation, 1-25-1, Nisisinjuku, Sinjuku-ku, Tokyo 160-91, Japan

SUMMARY

The response of very stiff structures, such as nuclear reactor buildings, to earthquake ground motion is significantly affected by radiation damping due to the soil-structure interaction. The radiation damping can be computed by Dr. H. Tajimi's vibration admittance theory or Dr. T. Kobori's dynamical ground compliance theory. In order to apply the values derived from these theories to the practical problems, comparative studies between theoretical results and experimental results concerning the soil-structure interaction, especially if the ground is rock, are urgently needed. However, experimental results for rock are less easily obtained than theoretical ones.

The purpose of this paper is to describe the harmonic excitation tests of a model foundation on rock and to describe the results of comparative studies.

Outline of the Tests

The model foundation was made of reinforced concrete. It was 12m in diameter and 5m high. The average value of shear wave velocity of the rock under the foundation was 1,400m/sec. The dimensionless frequency of the foundation was adjusted to 0.3-1.4, simulating the actual nuclear reactor buildings. A vibration generator, which operates in a frequency range up to 50Hz, was used for the tests. The maximum force from the vibrator was limited to 4t. The vibrator was set on the foundation. The horizontal (two directions) and vertical harmonic excitation tests were carried out. Displacements were measured by floor type and underground type transducers. Also, earth pressures were measured by mercury-containing earth pressure meters.

Results of the Tests and Analyses

The fundamental natural frequencies obtained from both the resonance and phase lag curves of displacements and earth pressures were 35Hz horizontally and more than 50Hz vertically. The earth pressure distribution approached the uniform pressure distribution in the case of horizontal excitation, while it did so to the pressure distribution of a rigid base in the case of vertical excitation.

Resonance curves obtained from the tests were compared with the analytical results, which were calculated by the response analysis of a lumped mass system with dynamic stiffness and dashpots, derived from Dr. H. Tajimi's theory. The results of the tests showed good agreement with the theoretical values.

The dynamic stiffness and radiation damping values are calculated from the measured records by two methods. The first method is to obtain the values from the relation between the inertia force, including excitation force, and measured displacement. The second method is to obtain the values from the relation between the total force of measured earth pressures and measured displacements. The values obtained by these methods showed good agreement with theoretical values.

From the forced vibration tests of a model foundation and the simulation analyses, the following conclusions were drawn. Good applicability of both theories to the foundation on rock was recognized and the results were useful for design purposes.

1. Introduction

Dynamic stiffness can be computed by some methods based on the half-space elastic theory. In the theoretical approach, the ground is assumed to be a perfectly "Idealized Solid" that is, a homogeneous, isotropic and semi-infinite elastic medium. But, actual ground is not such an "Idealized Solid" in general. So, in order to apply the values derived from these theories to the practical problems, comparative studies between theoretical results and experimental results, concerning soil-structure interaction, are needed.

2. Outline of the Tests

The model foundation was constructed on the site of Sendai nuclear power station in Japan. Fig.-1 shows the experimental site and model foundation. The foundation was made of reinforced concrete. It was 12m in diameter and 5m high. The physical properties of concrete and rock are given in Table 1.

Fig.-2 shows the arrangement of the displacement meters for horizontal (N-S direction) excitation. This arrangement is similar to that for E-W excitation and vertical excitation. Fig.-3 shows the arrangement of earth pressure meters.

3. Results of the Tests

Fig.-4 shows the resonance and phase lag curves of displacement for horizontal, (N-S direction) and vertical excitation. Fig.-5 shows the resonance and phase lag curves of earth pressure for horizontal (N-S direction) and vertical excitation. The curves obtained from E-W excitation were similar to the curves obtained from N-S excitation, in shape. From the results of the tests, it was recognized that the fundamental natural frequency obtained from both the resonance and phase lag curves of displacements and earth pressure were 35Hz horizontally and more than 50Hz vertically, and the difference in vibration level between the N-S direction and the E-W direction could not be found. So, in this paper, results of N-S excitation were adopted as typical results for horizontal excitation.

Fig.-6 shows the mode of dynamic displacement for horizontal excitation at a frequency of 35Hz. Maximum displacements of each point are shown by arrows. Broken lines show representative displacement obtained from the observed amplitudes and phase lags of each point.

Fig.-7 shows the distribution of dynamic earth pressure on the contact surface of the foundation and the ground. The maximum amplitude of each point is shown by arrows. Curved lines show the values calculated from the following equations. α , β and γ are factors of the equations obtained from experimental results using the least squares method.

Figs.-8, 9 show the mode of dynamic displacement and distribution of dynamic earth pressure for 50Hz. Experimental results for vertical excitation are shown in Figs. 10-13. Frequencies of excitation are 30Hz and 50Hz. The functions of stress distribution were assumed as in eq.1 and 2.

For horizontal and vertical motions

$$\tau, \sigma = R \left[\alpha + \beta \left(\frac{r}{R} \right)^2 + \gamma \left(\frac{r}{R} \right)^4 \right] \quad (1)$$

For rotational motions

$$\tau = R^2 \left(\frac{r}{R} \right) \left[\alpha + \beta \left(\frac{r}{R} \right)^2 + \gamma \left(\frac{r}{R} \right)^4 \right] \cos \phi \quad (2)$$

where, τ, σ are the observed shear stress and normal stress of each point. R is radius of the foundation. r and ϕ are coordinates of each point.

These figures show that the earth pressure distribution approached the uniform distribution in the case of horizontal excitation, while it approached the distribution of the rigid base in the case of vertical excitation. Figs.-14, 15, 16 show the relation between frequency of excitation and stress distribution for horizontal, rotational and vertical motion respectively. Stress slope (θ) is shown by broken lines. As the frequency of excitation approaches the resonance range the value increases. But the value divided by total force acting on the contact surface of foundation and ground (θ/F) does not increase. From these figures, it is recognized that the stress distribution mode at the contact surface was not affected by the frequency of excitation.

4. Results of Comparative Studies

4.1 Resonance curves

Fig.-17 shows resonance curves of displacement for horizontal excitation. In the figure, the solid lines show test values and broken lines show analytical results which were calculated from the response analysis of a lumped mass system with dynamic stiffness and dash-pots, derived from Dr. H. Tajimi's vibration admittance theory. In the calculation, earth pressure distributions were assumed to be uniform for horizontal motion and triangular for rotational motion. Fig.-18 shows the mathematical model adopted for the analysis.

Physical properties and constants used for the analysis are given in Table 1 and 2 respectively. This figure shows good agreement between experimental and theoretical results.

4.2 Dynamic Ground Stiffness

Dynamic stiffnesses were calculated from the measured records by two kinds of method as follows:

1) Dynamic Stiffness Obtained from Inertia Force and Displacements.

The first method is to obtain values from the relation between the inertia force, and measured displacement. The following equations of motion were employed for the foundation. Symbols used in these equations are illustrated in Figs.-19, 20. Dynamic stiffness for horizontal motion (K_H) and rotational motion (K_R) are obtained from eq.3. Vertical stiffness (K_V) is obtained from eq.4.

$$\begin{bmatrix} m & mH \\ mH & I \end{bmatrix} \begin{Bmatrix} \ddot{X} \\ \ddot{\theta} \end{Bmatrix} + \begin{bmatrix} K_H & 0 \\ 0 & K_R \end{bmatrix} \begin{Bmatrix} X \\ \theta \end{Bmatrix} = P \begin{Bmatrix} 1 \\ H_p \end{Bmatrix} \quad (3)$$

$$m\ddot{V} + K_V \cdot V = P \quad (4)$$

where, X , \ddot{X} are horizontal displacement and acceleration, θ , $\ddot{\theta}$ are rotational angle, and acceleration. m , I are mass and rotatory inertia of the foundation. H , H_p are the heights of the center of gravity and vibration generator, P is force of excitation. V , \ddot{V} are vertical displacement and acceleration.

2) Dynamic Stiffness Obtained from Earth Pressure and Displacements

The second method is to obtain values from the relation between the total force of measured earth pressures and measured displacements. The following equations of motion were employed. Dynamic stiffness K_H , K_R , K_V are obtained from eq.5.

$$\begin{bmatrix} K_H & 0 \\ 0 & K_R \end{bmatrix} \begin{Bmatrix} X \\ \theta \end{Bmatrix} = \begin{Bmatrix} Q \\ M \end{Bmatrix}, \quad K_V \cdot V = F \quad (5)$$

where, Q , M , F are shear force, moment and vertical force acting on the contact surface between the foundation and ground. They were obtained from earth pressure.

Figs.-21 to 26 show comparison of theoretical and experimental results for dynamic stiffness and damping. Theoretical results are derived from Dr. H. Tajimi's vibration admittance theory. In the calculation, two kinds of earth pressure distribution were assumed for each motion. Rigid base and uniform load were assumed for horizontal and vertical motion. Rigid base and triangular load were assumed for rotational motion. The damping factor (h) was calculated using eq.6.

$$h = (\sqrt{1 + 4\xi^2} - 1) / 2\xi \quad , \quad \xi = K_I / 2K_R \quad (6)$$

where, K_R , K_I are the real and imaginary parts of dynamic stiffness respectively. Experimental results were obtained by two kinds of method. Both of them are illustrated in the figure.

Figs.-21, 22 show the dynamic stiffness and the damping factor for horizontal motion. Experimental results obtained by method (1) do not show good agreement with other results for high frequencies. In the calculation, it was assumed that the foundation behaves as a rigid body. But by these figures it was recognized that this assumption, when used in the calculation, was not applicable for horizontal excitation at high frequencies.

Figs.23 to 26 show dynamic stiffness and damping factor for rotational and vertical motion. These figures show good agreement between the theoretical and experimental results, especially for vertical motion.

5. Conclusions

From the forced vibration tests on a model foundation on rock and the simulation analyses, the following conclusions were drawn.

- 1) The fundamental natural frequencies obtained from both the resonance and phase lag curves of displacement and earth pressure were 35Hz horizontally and more than 50Hz vertically.
- 2) The earth pressure distribution approached the uniform pressure distribution in the case of horizontal excitation, while it approached the pressure distribution of the rigid base in the case of vertical excitation.
- 3) The mode of earth pressure distribution at the contact surface of the foundation and ground was not affected by the frequency of excitation.
- 4) Resonance curves obtained from the tests showed good agreement with the theoretical results.
- 5) Dynamic stiffnesses and damping factors obtained from the tests showed good agreement with the theoretical results.

Good applicability of the theories to the foundation on rock was recognized, and the results were useful for design purposes.

Acknowledgments

The authors wish to express their thanks to Prof. T. Kobori of Kyoto University, and Prof. H. Tajimi of Nihon University for their helpful advice.

References

- [1] T. Kobori "Dynamic Response of Rectangular Foundations on an Elastic-Space". Proceedings of Japan National Symposium on Earthquake Engineering, (1962)
- [2] H. Tajimi "Basic Theories on Aseismic Design of Structures". Report of the Institute of Industrial Science, University of Tokyo, Vol.8 No. 4, (1959)

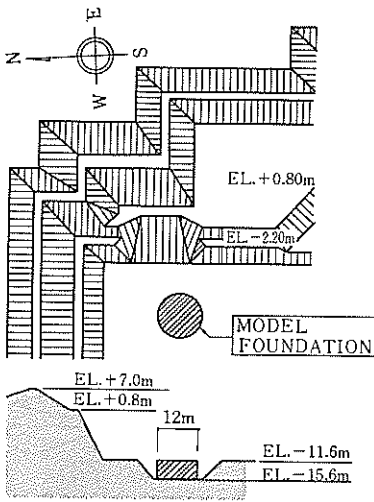


Fig.1 Experimental site and model foundation

Table.1 Physical properties of concrete and rock

Concrete	Young's modulus	$E = 3.0 \times 10^5 \text{ kg/cm}^2$
	Poisson's ratio	$\nu = 0.167$
	Normal strength per unit area	$F_c = 387 \text{ kg/cm}^2$
Rock	Shear wave velocity	$V_s = 1400 \text{ m/sec.}$
	Modulus of rigidity	$G = 5.4 \times 10^5 \text{ t/m}^2$
	Young's modulus	$E = 1.47 \times 10^9 \text{ t/m}^2$
	Poisson's ratio	$\nu = 0.36$
	Density	$\gamma = 2.7 \text{ t/m}^3$

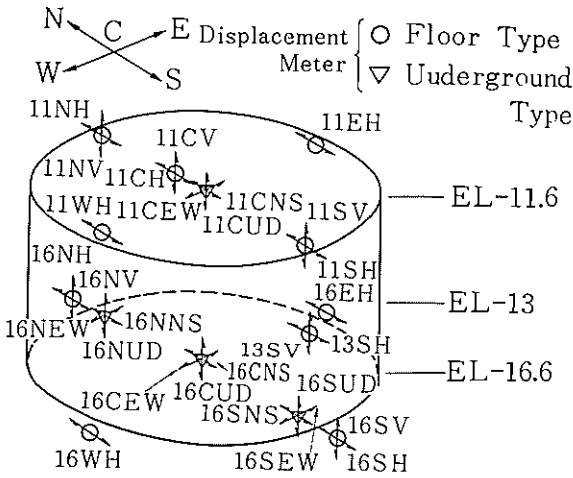


Fig.2 Arrangement of displacement meters for horizontal excitation

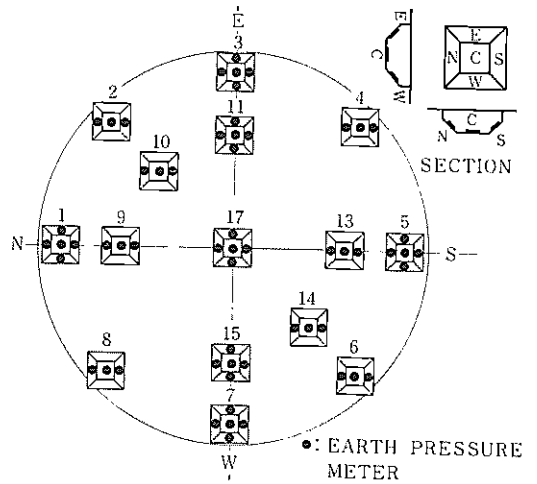


Fig.3 Arrangement of earth pressure meters

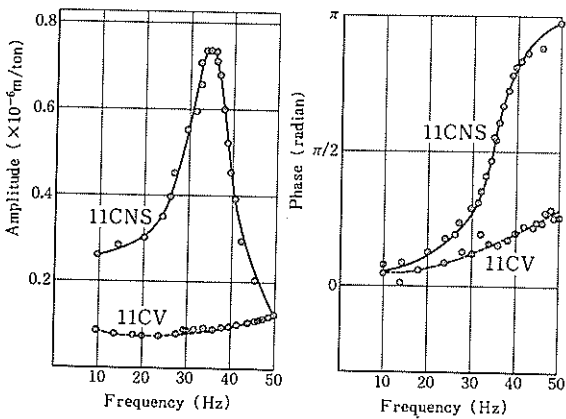


Fig.4 Resonance and phase lag curves of displacement

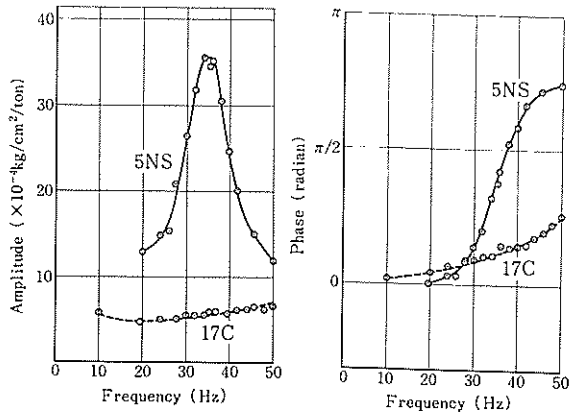


Fig.5 Resonance and phase lag curves of earth pressure

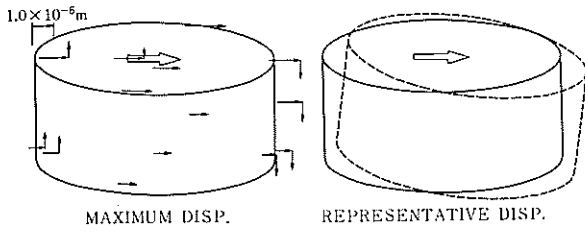


Fig.6 Mode of dynamic displacement for horizontal excitation (35Hz)

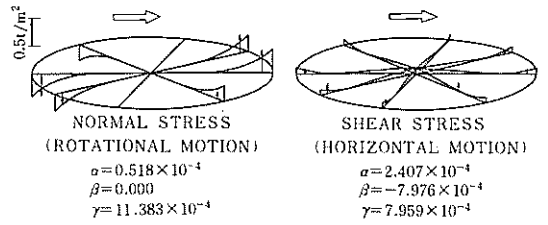


Fig.7 Distribution of dynamic earth pressure for horizontal excitation (35Hz)

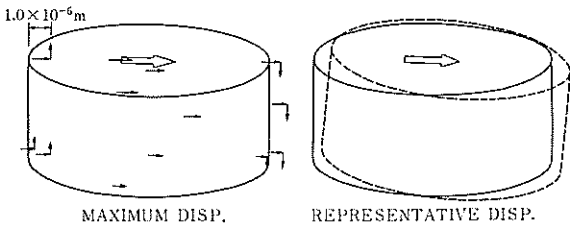


Fig.8 Mode of dynamic displacement for horizontal excitation (50Hz)

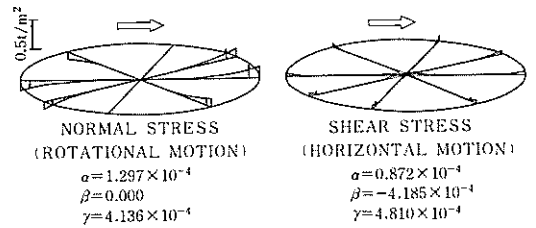


Fig.9 Distribution of dynamic earth pressure for horizontal excitation (50Hz)

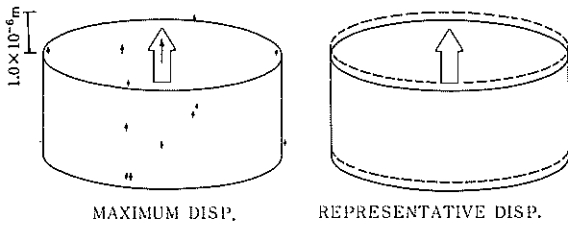


Fig.10 Mode of dynamic displacement for vertical excitation (30Hz)

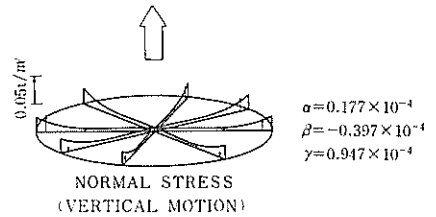


Fig.11 Distribution of dynamic earth pressure for vertical excitation (30Hz)

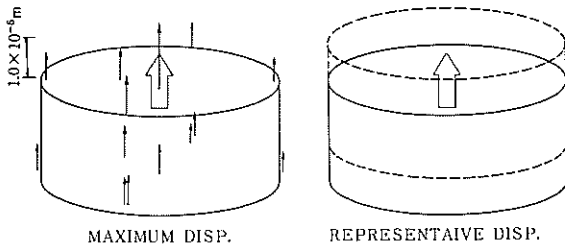


Fig.12 Mode of dynamic displacement for vertical excitation (50Hz)

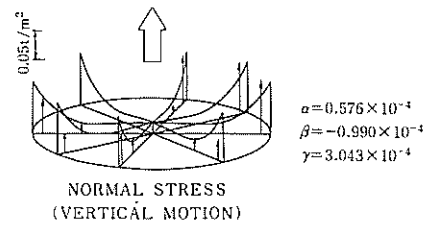


Fig.13 Distribution of dynamic earth pressure for vertical excitation (50Hz)

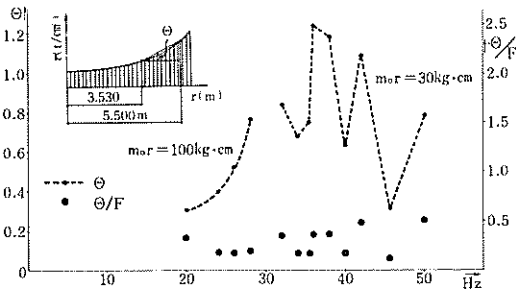


Fig.14 Relation between frequency of excitation and stress distribution for horizontal motion

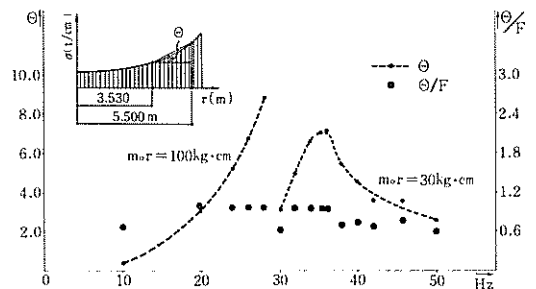


Fig.15 Relation between frequency of excitation and stress distribution for rotational motion

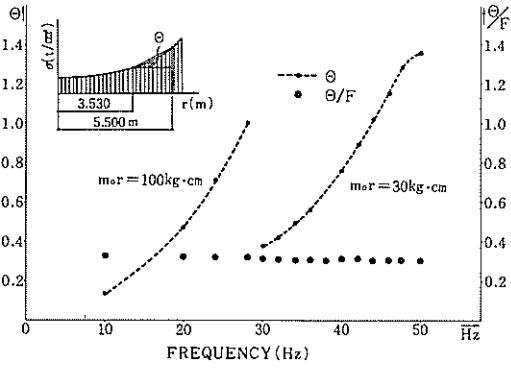


Fig.16 Relation between frequency of excitation and stress distribution for vertical motion

Table.2 Constants used for mathematical model

Weight	$W_1 = 339.3 \text{ ton}$
	$W_2 = 678.6 \text{ ton}$
	$W_3 = 339.3 \text{ ton}$
	$I_m = 23,523.9 \text{ t}\cdot\text{m}^2$
Section (K_1 K_2)	$A_N = 113.1 \text{ m}^2$
	$A_S = 99.0 \text{ m}^2$
	$I = 1,017.9 \text{ m}^4$
K_R, K_S	Dynamic stiffness derived from Dr. H. Tajimi's Vibrational admittance theory. (Ref. Fig. 21 ~ Fig. 26)

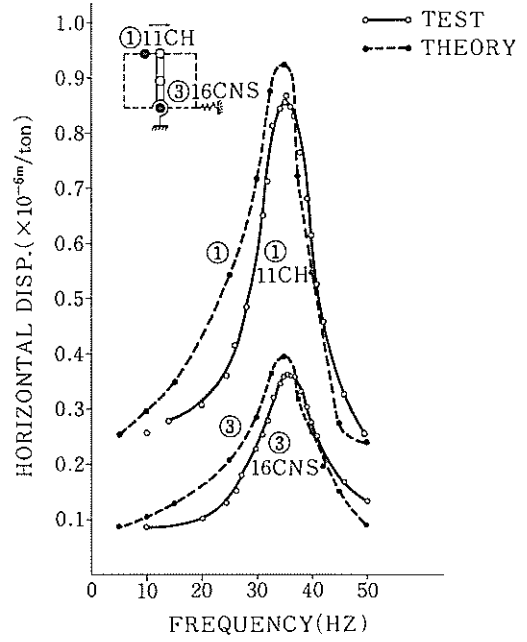


Fig.17 Comparison of theoretical and experimental results for resonance curves

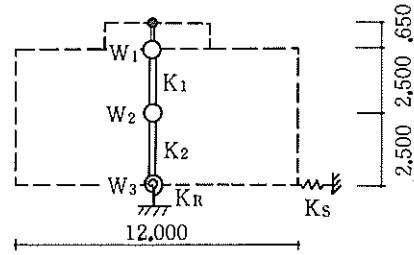


Fig.18 Mathematical model

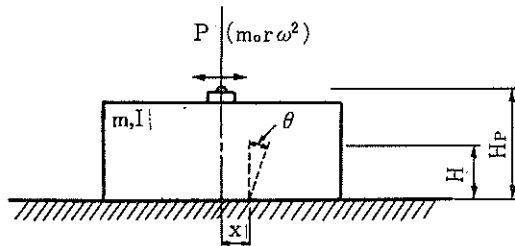


Fig.19 Explanation of symbols used for eq. (3)

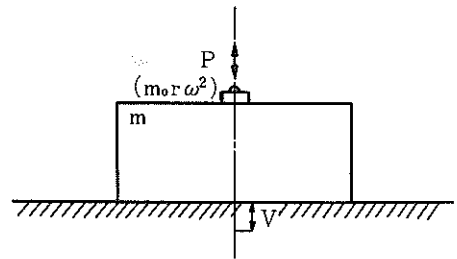






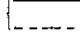



Fig.20 Explanation of symbols used for eq. (4)

TEST  BY METHOD (1)
 BY METHOD (2)
 THEORY  RIGID BASE
 UNIFORM L.

TEST  BY METHOD (1)
 BY METHOD (2)
 THEORY  RIGID BASE
 UNIFORM L.

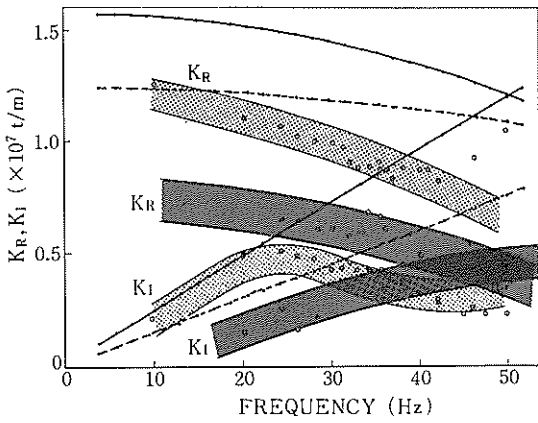


Fig. 21 Dynamic stiffness for horizontal motion

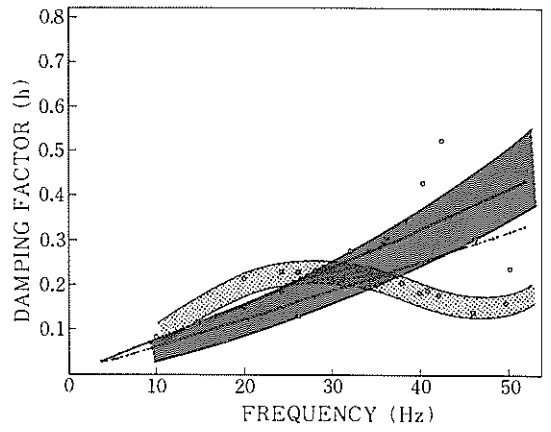


Fig. 22 Damping factor for horizontal motion

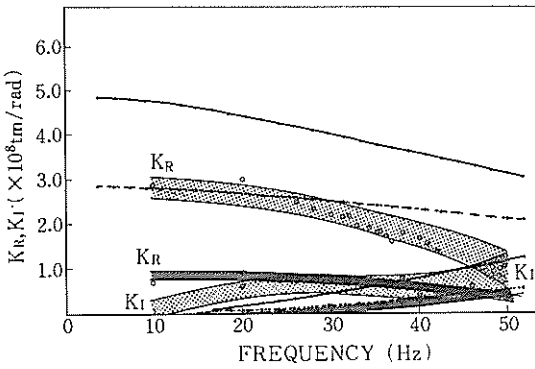


Fig. 23 Dynamic stiffness for rotational motion

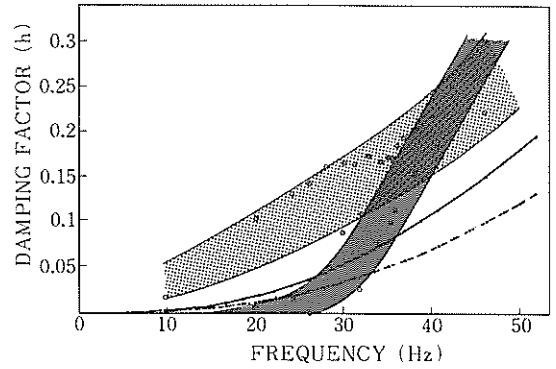


Fig. 24 Damping factor for rotational motion

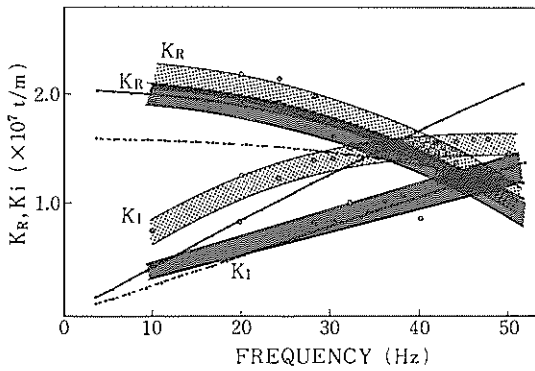


Fig. 25 Dynamic stiffness for vertical motion

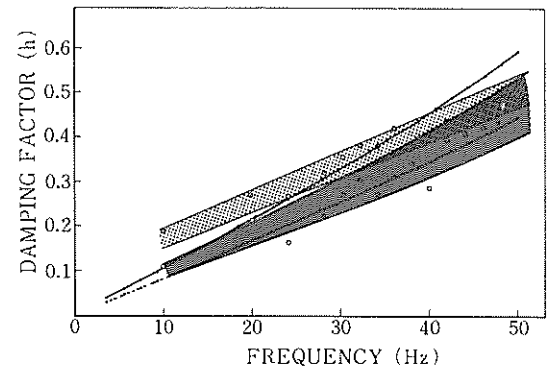


Fig. 26 Damping factor for vertical motion